

A Model Based Control methodology combining Blade Pitch and Adaptive Trailing Edge Flaps in a common framework

L. C. Henriksen
DTU Wind Energy
DK-4000 Roskilde, Denmark
larh@dtu.dk

L. Bergami
DTU Wind Energy
DK-4000 Roskilde, Denmark
leob@dtu.dk

P. B. Andersen
DTU Wind Energy
DK-2800 Kgs. Lyngby, Denmark
pbja@dtu.dk

Abstract:

This work investigates how adaptive trailing edge flaps and classical blade pitch can work in concert using a model-based state space control formulation. The trade-off between load reduction and actuator activity is decided by setting different weights in the objective function used by the model-based controller. The combined control approach allow to achieve higher load alleviations, furthermore, in the presence of e.g. deterioration of an actuator, it enables an online re-tuning of the workload distribution of blade pitch and trailing edge flaps, thus potentially increasing the smart rotor reliability.

Keywords: aeroelasticity, active load control, smart rotor

1 Introduction

Wind turbines are constantly exposed to unsteady loads due to turbulence and gusts in the incoming flow and this increases significantly the cost. Therefore, researchers and industry are aimed at finding technical solutions that can alleviate the loads on the turbines. Local control of the aerodynamic forces along the blade span, as well as active pitching of the whole blade, can be used to compensate for the variations in the incoming flow, and thus reduce the loads arising on the turbine rotor, a concept often referred to as *smart-rotor* [1]. Local aerodynamic control with Adaptive Trailing Edge Flaps (ATEF) with a smooth and continuous deformation shape has been under development in several research institutions; the load alleviation potential is confirmed by several aeroelastic simulations [2–6], and experiments [7, 8].

Most of the investigations documented in the literature follow a control design approach where the turbine power control part is developed separately from the active load alleviation control, which is often designed in a second phase and exclusively manages the flap activity. Mutual interference between the two control algorithms is then avoided by frequency separation, with the power control targeting low frequency variations, and the active load control

the rest of the range. This paper presents an innovative control design approach, where both load alleviation and power control objectives are managed by the same model based control algorithm, which returns the control signals for the turbine generator torque, for the blade pitch angles, and for the deflection of the adaptive trailing edge flaps (ATEF) distributed along the blades. The control problem is solved in a model predictive formulation, where the control design model is retrieved from first principles.

The proposed control algorithm is applied to the NREL 5 MW reference turbine [9] in a smart rotor configuration with ATEF; the turbine response is simulated with the aero-servo-elastic code HAWC2 [10]. The paper is structured as follows: the control design model is presented in Section 2, with particular focus on the modeling of the Adaptive Trailing Edge Flap (ATEF) contributions. A brief introduction to the controller is found in Section 3. Finally, results are presented and discussed in Section 5 and conclusions are drawn in Section 6.

2 Model for controller design

The control design model is derived from first principles considerations, and follows a similar formulation to the one presented in Henriksen et al. [11]. The structural model includes: 1 drive-shaft torsion degrees of freedom (DOF), 1 tower fore-aft DOF, 1 tower side-side DOF, 2 blade edgewise and 2 flap-wise DOFs. Furthermore the blade-wide turbulent wind speed as well as the induced wind speed normal to the rotor plane is included in the control design model.

The aerodynamic part of the model is extended to include the effect deformable trailing edge flaps. In Henriksen et al. [11] the lift and drag coefficients, C_l and C_d , are only functions of the angle of attack α ; the model is now extended to include dependency on the ATEF angle β , [12]. In the model used in this work, the effect is approximated as a linear effect:

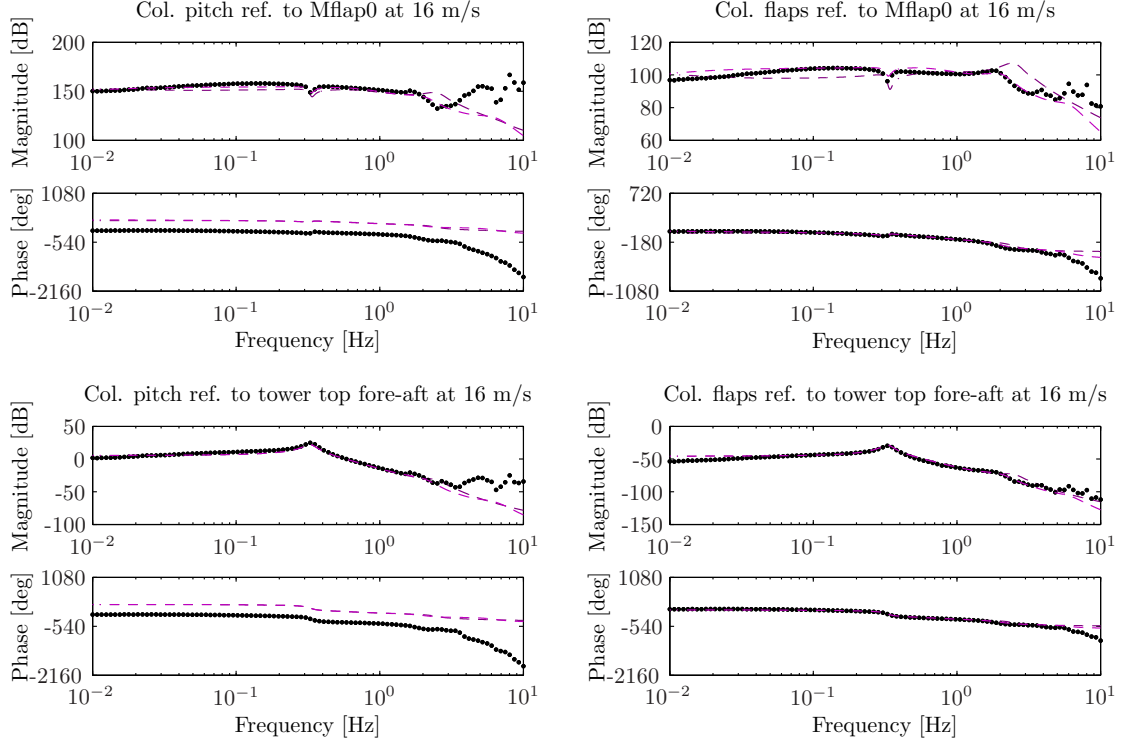


Figure 1: Bode plots of the frequency response at a mean wind speed of 16 m/s, comparison of the response given by the linearized model (dashed lines) with the response simulated by the aeroelastic code HAWC2 (black dots).

$$C_l(\alpha, \beta) \approx C_l(\alpha, 0) + \frac{\partial C_l(\alpha, 0)}{\partial \beta} \beta \quad (1)$$

$$C_d(\alpha, \beta) \approx C_d(\alpha, 0) + \frac{\partial C_d(\alpha, 0)}{\partial \beta} \beta \quad (2)$$

The change in lift and drag forces cause a change in induction factors, which are now function of pitch angle θ , tip-speed ratio λ , and flap deflection β . The dependency on the flap deflection is also simplified by a linear approximation:

$$a_n(\theta, \lambda, \beta) \approx a_n(\theta, \lambda, 0) + \frac{\partial a_n(\theta, \lambda, 0)}{\partial \beta} \beta \quad (3)$$

$$a_t(\theta, \lambda, \beta) \approx a_t(\theta, \lambda, 0) + \frac{\partial a_t(\theta, \lambda, 0)}{\partial \beta} \beta \quad (4)$$

The control model is then transformed from a time-varying system to a linear time-invariant system using the Coleman transform [13]. The correct implementation of the linearized model, and its ability to capture the relevant system dynamics are verified by comparing the frequency response predicted by the linear model against the response simulated with the multi-body time-marching aeroelastic code HAWC2. Figure 1 reports the corresponding Bode plots of the frequency response from harmonic pitch actions (on the left column), and from harmonic flap deflection (right column); the response is measured at the

blade root flapwise bending moment (first row), and at the tower top acceleration in the fore-aft direction (second row). The linearized model used in the control formulation (response indicated by the dashed lines) is able to describe sufficiently well the dynamics of the system to be controlled, especially in the low frequency region.

3 Controller

The controller presented in the work is based on the one described by Henriksen et al. [11], further extended to include Adaptive Trailing Edge Flap control. The controller setup is sketched in Figure 2, where an extended Kalman filter estimates the states of the control design using the following set of sensors:

- Pitch angle of each blade
- Generator torque
- Generator power
- Generator speed
- Rotor Speed
- Tower top fore-aft acceleration
- Tower top side-side acceleration

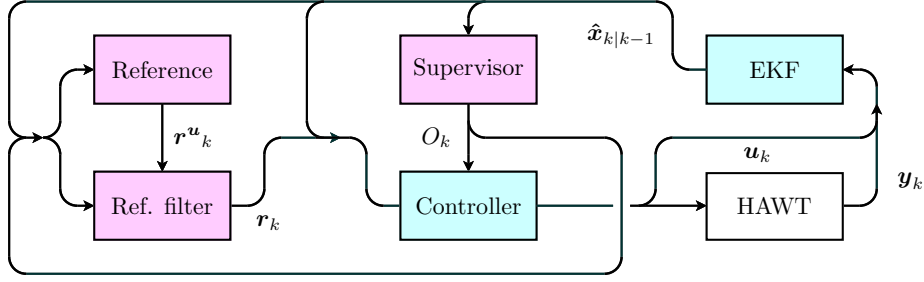


Figure 2: Setup of the hybrid controller. An extended Kalman filter (EKF) provides estimates of states used by other blocks in the diagram. Supervisor block provides partial or full load control objectives to controller depending on switching conditions. Reference and reference filter blocks provide references for the controller to track depending on whether partial or full load operation is active.

- Flapwise blade root bending moment of each blade
- Edgewise blade root bending moment of each blade

The estimated states are used by a Model Predictive Control algorithm, which calculates the optimal control actions that minimizes a cost function that includes the following weight elements:

- Weight on generator power
- Weight on generator speed
- Weight on tower top fore-aft velocity
- Weight on tower top side-side velocity
- Frequency dependent weight on collective pitch angle
- Frequency dependent weight on cyclic pitch angles
- Frequency dependent weight on generator torque
- Frequency dependent weight on collective ATEF
- Frequency dependent weight on cyclic ATEF: *Weight ATEF act.*
- Weight on cyclic flapwise blade root bending moments: *Weight ΔM_x Cycl.*

The weight on the last two elements of the cost function will be varied in the following investigations, so to explore different control configurations and combinations of pitch and flap activity.

4 Test Case

The NREL 5 MW baseline wind turbine in its on-shore configuration is taken as reference model for

the aeroelastic simulations presented in this work. The wind turbine, thoroughly described by Jonkman et al. [9], is representative of modern multi-megawatt models, it has a three bladed rotor of 126 m diameter with upwind orientation, variable speed and pitch-to-feather control. Jonkman et al. [9] also define a baseline PI control algorithm, where power regulation above rated is obtained by collective blade pitch actions based on low pass filtered measurements of the drive train speed. The load results obtained with the baseline PI control will be used as a term of reference in the following analysis.

The turbine rotor is equipped with adaptive trailing edge flaps, which extend for 10 % of the airfoil chord and cover 20 % of the blade length, from 47.7 m to 60.0 m span. The maximum flap deflection is limited to $\pm 10^\circ$, resulting in maximum steady lift coefficient variations of ± 0.42 . All the flaps on the same blade are controlled by the same signal, and no constraints are applied on the flap maximum deflection speed; nevertheless, the frequency weighting on the control cost function inhibits high frequency activity of the flap, thus giving flap deflection signals that very rarely require maximum deflection rates above 50 deg/s. The pitch and generator actuator dynamics are modeled as second and first order low pass filters, respectively.

Aeroelastic simulations are performed with the HAWC2 code [10], reproducing the wind field conditions prescribed by the IEC standard [14] for a class A turbine. In this paper, only results referring to mean wind speed 18 m/s are considered, and a total of 40 minutes (4 x 10 minutes seeds) turbulent wind is simulated for each control configuration.

5 Results

The performances of the combined model based control are investigated by running aeroelastic simulations of the NREL 5 MW turbine under different control weight configurations. Several combinations

of pitch and flap activity are obtained by acting on two weight parameters in the control cost function introduced in section 3:

- *Weight ATEF act.* determines the penalization imposed on the flap activity. Low values corresponds to a control setting that favor the flap activity, whereas high values favor the blade pitch action.
- *Weight ΔM_x Cycl.* determines the penalization on cyclic variation of the blade root flapwise bending moment. Higher values indicate a control configuration that focuses more on blade root flapwise bending moment alleviation.

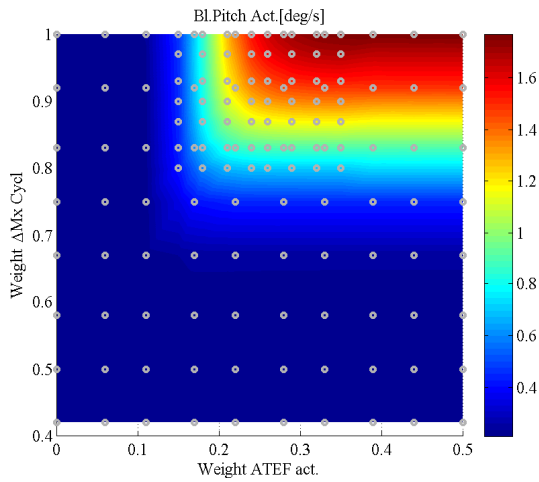


Figure 3: Blade pitch activity for different combinations of the control cost function weights. The actuator activity is measured as the total traveled distance (in degrees), normalized by the simulation time.

The blade pitch and ATEF activities are quantified as the total distance traveled by the actuators (in degrees), then normalized by the simulation time. The activity registered with the investigated control weight combinations is reported in figure 3 for the blade pitch, and figure 4 for the flap. As expected, the highest pitch activity (dark red color in fig. 3) occurs for weight settings that penalize flap action (high *ATEF act.* weights), and focus on cyclic load alleviation (high ΔM_x Cycl weights); as a term of reference, the pitch activity with the NREL 5 MW baseline PI controller is around 0.3 deg/s, at the bottom of the color scale. High flap activity is obtained with high ΔM_x Cycl weights, and low *ATEF act.* penalization; the gray circles in the plots mark the weight combinations where simulations were actually performed.

Load alleviation performances of the combined control system are measured in terms of fatigue Damage Equivalent Loads (DEL), which are computed under Palmgren-Miner linear damage assumption by applying rain-flow counting to the simulated

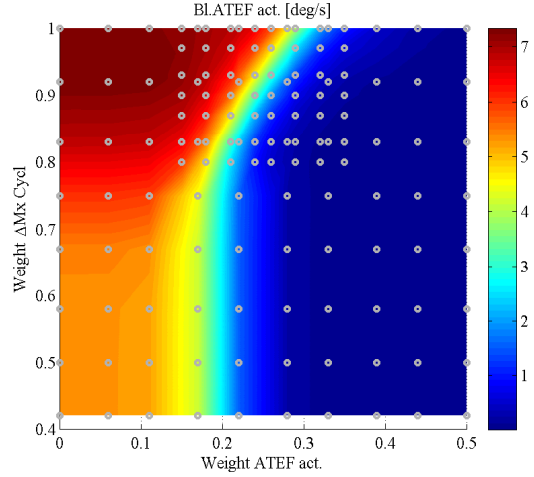


Figure 4: Adaptive Trailing Edge Flap activity for different combinations of the control cost function weights. The actuator activity is measured as the total traveled distance (in degrees), normalized by the simulation time.

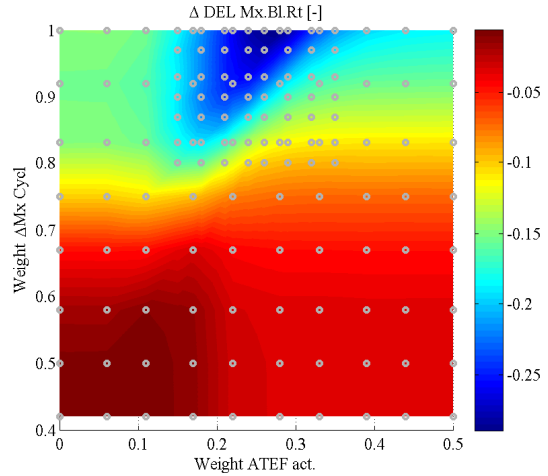


Figure 5: Performance of the active control in terms of alleviation of Fatigue Damage Equivalent Loads (DEL) at the blade root flapwise bending moment, Wöhler curve exponent of 10. Results given as percentage variation from the DEL measured on the baseline NREL 5 MW turbine with its standard PI controller [9]; simulations are performed in the points indicated by the gray circles.

time series; a Wöhler curve fatigue exponent of 10 is used for the blade DEL, and an exponent of 4 for the tower loads. The load alleviation is expressed as the DEL difference between the active load control case, and the reference baseline one; negative values thus indicate a reduction of fatigue loads. The difference is then normalized by the DEL in the reference case. Among the investigated control weight combinations, higher fatigue load alleviation on the blade root flapwise bending moment are obtained by

increasing the weight on the bending moment cyclic variation, and the highest DEL alleviation is achieved by using a combination of both flap and pitch control actions, dark blue area in figure 5.

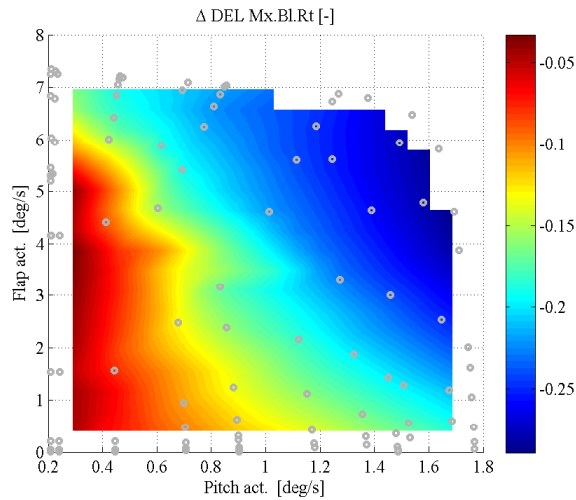


Figure 6: Fatigue Damage Equivalent Loads (DEL) alleviation at the blade root flapwise bending compared to the baseline NREL 5 MW turbine, Wöhler curve exponent of 10. The load alleviation is plotted as a function of both the blade pitch actuator traveled distance (horizontal axis), and the flap actuator traveled distance (vertical axis). Simulation data are only available for the points indicated by the gray circles.

A more informative display of the controller performances is obtained by remapping the load alleviation results as a function of both the blade pitch and the flap activity, figure 6. The plot immediately highlights that larger load alleviations require higher control activity, either with pitch or flap actuators. Active load alleviation with exclusively blade pitch actuators reaches to 18-20 % DEL reduction, whereas lower figures (approximately 15 %) are achieved when the flap actuators alone target the cyclic loads, a result in-line with previous investigations featuring similar smart rotor setups [6]. The highest load alleviation performances are achieved when the controller employs a combination of both the blade pitch and the flap actuators: load alleviation is increased from 18 % for the pitch alone, to nearly 30 % for the combined control actions.

Another advantage of the combined control formulation lies in the possibility of one actuator to partly take over and reduce the work load of the other. For instance, actively reducing the DEL by 16 % with blade pitch alone would require an average activity of 1.5° pitch variation every second of operation; by including flap action in the task, the work load on the pitch actuator is lowered down to one third, without compromising on the DEL alleviation. The possibility of one actuator relieving the work load of the other could be exploited to decrease actuator wear, and

eventually postpone maintenance operations.

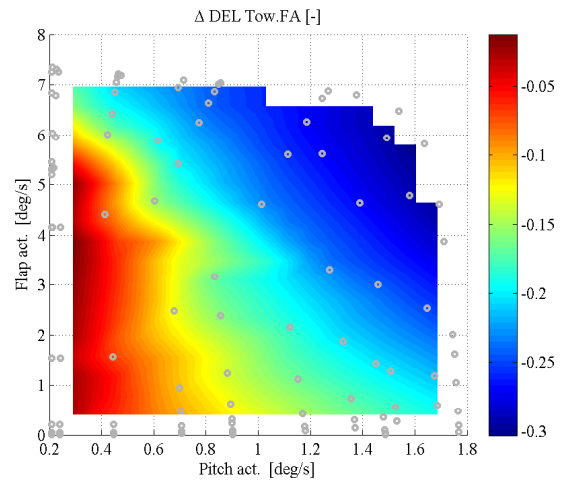


Figure 7: Fatigue Damage Equivalent Loads (DEL) alleviation at the tower bottom flange fore-aft bending moment compared to the baseline NREL 5 MW turbine, Wöhler curve exponent of 4. Simulation data are only available for the points indicated by the gray circles.

To avoid increasing the loads on the tower as a consequence of the alleviation on the rotor, estimations of the tower top velocities are included in the control cost function, section 3. The model based control algorithm is thus able to reduce at the same time the loads on the blades, and at the tower bottom flange: in the fore-aft direction fatigue DEL alleviation up to 30 % are achieved, with a distribution similar to the one observed for the blade root flapwise DEL, figure 7.

6 Conclusion

The paper presented an algorithm that combines generator torque, blade pitch, and adaptive trailing edge flaps in the same model predictive control framework. The control model is retrieved from first principle models of the turbine structural components and from a linearized BEM-based aerodynamic formulation; comparisons of the frequency response predictions with the results from aeroelastic simulations show that the control linear model is able to describe the dominant system dynamics.

The performances of the proposed control algorithm are evaluated in terms of fatigue damage equivalent loads alleviation on the NREL 5 MW reference turbine, with a smart rotor configuration featuring flaps on the outer 20 % span of the blades. Aeroelastic simulations have highlighted some advantages of a model based control strategy able to combine and supervise both flap and pitch activity:

- Higher fatigue load alleviation is achieved by

combining flap and pitch control actions. Reduction of fatigue damage equivalent loads (DEL) in the blade root flapwise bending moment up to 30 % are reported when both pitch and flap are in use; in comparison, active alleviation with either flap or pitch actions alone bring DEL reductions of 15 % and 18 %, respectively.

- The combined framework allows to shift the control activity required for load alleviation between the pitch and the flap actuators. By including flap actions, the blade pitch workload, and thus the actuator wear, is significantly reduced, while still achieving the same reduction of fatigue damage.

Fatigue damage at the tower bottom flange is also reduced by active load alleviation, the variation of the tower fore-aft DEL from the reference case shows a maximum reduction close to 30%, and an overall trend similar to the blade flapwise load alleviation.

The combined model based control methodology proved rather powerful and efficient in pursuing the blade and tower load alleviation objectives; future work should consider extending the methodology to other objectives, as, for instance, increase of power capture below rated conditions, or reduction of the drive train loads and generator speed variations. Independent flap actuators and sensors distributed along the blade span are other topics that might be worth consider in future investigations.

References

- [1] T. K. Barlas and G. van Kuik. State of the art and perspectives of smart rotor control for wind turbines. *Journal of Physics: Conference Series*, 75(1):012080 (20 pp.), 2007.
- [2] T. Buhl, M. Gaunaa, and C. Bak. Potential load reduction using airfoils with variable trailing edge geometry. *Transactions of the ASME. Journal of Solar Energy Engineering*, 127(4):503–516, 2005.
- [3] Peter Bjoern Andersen, Lars Henriksen, Mac Gaunaa, Christian Bak, and Thomas Buhl. Deformable trailing edge flaps for modern megawatt wind turbine controllers using strain gauge sensors. *Wind Energy*, 13(2-3):193–206, March 2010.
- [4] Matthew A. Lackner and Gijs van Kuik. A comparison of smart rotor control approaches using trailing edge flaps and individual pitch control. *Wind Energy*, 13(2-3):117–134, March 2010.
- [5] D.G. Wilson, B.R. Resor, D.E. Berg, T.K. Barlas, and G.A.M. van Kuik. Active aerodynamic blade distributed flap control design procedure for load reduction on the UpWind 5MW wind turbine. In *Proceedings of the 48th AIAA Aerospace Sciences Meeting*, page 407, 2010.
- [6] T. K. Barlas, G. J. van der Veen, and G. A.M. van Kuik. Model predictive control for wind turbines with distributed active flaps: incorporating inflow signals and actuator constraints. *Wind Energy*, Early view (published on-line), 2011.
- [7] Damien Castaignet, Jens Jakob Wedel-Heinen, Taeseong Kim, Thomas Buhl, and Niels Poulsen. Results from the first full scale wind turbine equipped with trailing edge flaps. In *Proceedings of 28th AIAA Applied Aerodynamics Conference*, Chicago, IL (US), June 2010. American Institute of Aeronautics and Astronautics.
- [8] T.k. Barlas, W. van Wingerden, A.w. Hulskamp, G.a. M. van Kuik, and H.e. N. Bersee. Smart dynamic rotor control using active flaps on a small-scale wind turbine: aeroelastic modeling and comparison with wind tunnel measurements. *Wind Energy*, Early View (published on-line):n/a–n/a, 2012.
- [9] J. Jonkman, S. Butterfield, W. Musial, and G. Scott. Definition of a 5-MW reference wind turbine for offshore system development. Technical Report NREL/TP-500-38060, National Renewable Energy Laboratory, 1617 Cole Boulevard, Golden, Colorado 80401-3393, February 2009.
- [10] T. J. Larsen and A. M. Hansen. How 2 HAWC2, the user's manual. Technical Report Risø-R-1597(ver. 3-1)(EN), Risø National Laboratory, 2007.
- [11] Lars Christian Henriksen, Morten Hartvig Hansen, and Niels Kjølstad Poulsen. Beyond the cp-curve in model-based control of wind turbines. In *Scientific Proceedings of EWEA 2012 - European Wind Energy Conference & Exhibition*, pages 147–152, Copenhagen, Denmark, April 2012. EWEA - The European Wind Energy Association.
- [12] Leonardo Bergami and Mac Gaunaa. ATEFlap aerodynamic model, a dynamic stall model including the effects of trailing edge flap deflection. Technical Report R-1792(EN), Risoe National Laboratory. Technical University of Denmark, Roskilde, Denmark, February 2012.
- [13] G. Bir. Multi-blade coordinate transformation and its application to wind turbine analysis. In *46th AIAA aerospace sciences meeting and exhibit*, Reno, NV., 2008.

- [14] IEC/TC88. *IEC 61400-1 Ed.3: Wind turbines - Part 1: Design requirements*. International Electrotechnical Commission (IEC), 8 2005.